Applications of Mathematics

Larisa Beilina; Sergey Korotov; Michal Křížek

Nonobtuse tetrahedral partitions that refine locally towards Fichera-like corners

Applications of Mathematics, Vol. 50 (2005), No. 6, 569–581

Persistent URL: http://dml.cz/dmlcz/134624

NONOBTUSE TETRAHEDRAL PARTITIONS THAT REFINE LOCALLY TOWARDS FICHERA-LIKE CORNERS*

Larisa Beilina, Basel, Sergey Korotov, Helsinki,
and Michal Křížek, Praha

(Received March 5, 2004)

Dedicated to Prof. Qun Lin on the occasion of his 70th birthday

Abstract. Linear tetrahedral finite elements whose dihedral angles are all nonobtuse guarantee the validity of the discrete maximum principle for a wide class of second order elliptic and parabolic problems. In this paper we present an algorithm which generates nonobtuse face-to-face tetrahedral partitions that refine locally towards a given Fichera-like corner of a particular polyhedral domain.

Keywords: partial differential equations, finite element method, path tetrahedron, linear tetrahedral finite element, discrete maximum principle, reentrant corner, Fichera vertex, nonlinear heat conduction

MSC 2000: 65N30, 65N50, 51M20

1. Introduction

Linear tetrahedral finite elements are commonly used for solving elliptic and parabolic problems. The structure and properties of the associated stiffness matrices essentially depend on the dihedral angles between the faces of those elements. In order to see this, let us consider an arbitrary tetrahedron $ABCD$. Let p and q be two linear nodal basis functions such that

$$p(A) = 1, \quad p(B) = p(C) = p(D) = 0,$$
$$q(B) = 1, \quad q(A) = q(C) = q(D) = 0.$$

* The first author was supported by the Swedish Foundation for Strategic Research, the second author was supported by Grant No. 49051 of the Academy of Finland, the third author was supported by Grant No. A 1019201 of the Academy of Sciences of the Czech Republic and by Institutional Research Plan AV0Z 10190503.

Then a straightforward calculation leads to the following formula (see [22, p. 63])

$$\nabla p \cdot \nabla q = -\frac{\operatorname{meas}_2 ACD \operatorname{meas}_2 BCD}{9(\operatorname{meas}_3 ABCD)^2} \cos\alpha, \tag{1.1}$$

where α is the angle between the faces ACD and BCD (see Fig. 1) and the symbol meas_d stands for the d-dimensional measure. The scalar product in (1.1) is independent of all the other 5 dihedral angles. If $\alpha > \pi/2$, then the scalar product in (1.1) is obviously positive. Hence, each obtuse dihedral angle of the tetrahedron $ABCD$ gives a positive contribution to the corresponding off-diagonal entry of the element (and also global) stiffness matrix, when solving the Poisson problem.

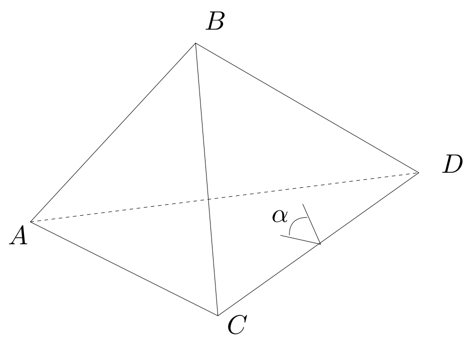

Figure 1. A general tetrahedron whose two faces include the angle α.

Note that the same is also true for a wide class of nonlinear elliptic problems of the form (see [22])

$$-\nabla \cdot (\lambda(x, u, \nabla u)\nabla u) = f(x) \quad \text{in } \Omega, \tag{1.2}$$

$$u = 0 \quad \text{on } \partial\Omega, \tag{1.3}$$

where λ is a uniformly positive smooth function and Ω is a bounded polyhedral domain with a Lipschitz-continuous boundary $\partial\Omega$. Equations (1.2)–(1.3) describe, for instance, a stationary nonlinear heat conduction or fluid flow problems.

Recall that a tetrahedron is said to be *nonobtuse* if all six dihedral angles between its faces are less than or equal to $\pi/2$. In this paper, we shall use only face-to-face tetrahedral partitions of $\overline{\Omega}$, which are called, for simplicity, *partitions*. A partition is said to be *nonobtuse* if it only contains nonobtuse tetrahedra.

According to [22], linear elements applied to problem (1.2)–(1.3) on nonobtuse partitions yield irreducibly diagonally dominant stiffness matrices (whose off-diagonal entries are all nonpositive). It is well known (see [8, Chapt. II.4.3] or [29, p. 85]) that such matrices are monotone. This makes it possible to prove easily L^∞-convergence of the finite element method like in [13], where a two-dimensional nonlinear problem was solved on nonobtuse triangulations. Nonobtuse tetrahedral partitions also guarantee the validity of the discrete maximum principle for problem (1.2)–(1.3), i.e., we have $u_h \leqslant 0$ provided $f \leqslant 0$, where u_h is the unique Galerkin approximation (see [22]) of the solution of (1.2)–(1.3). In other words, u_h attains its maximum on the boundary $\partial\Omega$ if homogeneous Dirichlet boundary conditions and nonpositive right-hand sides are considered. For results on the validity of the discrete maximum principle for parabolic problems on nonobtuse simplicial meshes, we refer to [15].

In [18], we gave a global refinement procedure yielding nonobtuse tetrahedra over the whole domain. However, this technique requires a large amount of computer time and memory to store the associated stiffness matrix. Therefore, in the present paper we introduce a local partitioning procedure yielding nonobtuse partitions that refine only near a particular vertex, where a singularity of the exact solution may appear (see [12], [28]). Note that the standard red-green refinement techniques (see, e.g., [6], [20], [23], [24], [27]) do not yield nonobtuse partitions in general, since they use bisections. Other local refinement algorithms proposed in [7] and [16] do not produce nonobtuse tetrahedra either. Several mesh refinement strategies of anisotropic meshes (see [2], [3]) or refinement techniques based on Zienkiewicz-Zhu estimator (see [25], [26]) also do not yield nonobtuse tetrahedra, and therefore, the discrete maximum principle need not be valid.

Note also that the discrete maximum principle can be violated for standard trilinear block finite elements (see [21, p. 562]) and also for bilinear rectangular elements (see [4, p. 254]). This is the reason why simplicial (triangular or tetrahedral) elements may be preferable.

In Section 2, we recall the definition of a special tetrahedron—a path tetrahedron—and show how to generate nonobtuse partitions that locally refine near one of its vertices. In Section 3, we generalize this refinement procedure to a neighborhood of Fichera-like corners. Section 4 is concerned with several numerical tests.

2. Nonobtuse tetrahedral partitions of a path tetrahedron

Definition 2.1. A tetrahedron is said to be a *path tetrahedron* if it has three mutually perpendicular edges which do not pass through the same vertex.

The reason for the name of the above tetrahedron is that its three perpendicular edges form a "path" (see [5]).

Proposition 2.2. *Any path tetrahedron is nonobtuse.*

Proof. For the proof see [18, p. 728–729]. □

A typical example of a path tetrahedron is illustrated in Fig. 2 (all its right angles, solid and dihedral, are indicated there). The nonintersecting edges AB and CD are also perpendicular, which means that the three-component vectors $\overrightarrow{AB}$ and $\overrightarrow{CD}$ are orthogonal.

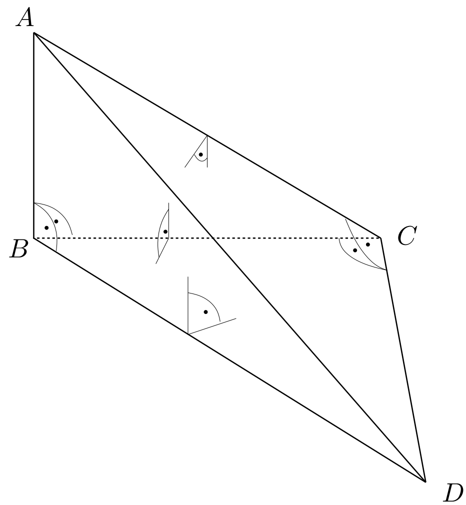

Figure 2. A path tetrahedron.

Definition 2.3. An infinite set of partitions is said to be *regular* if there exists a constant $C > 0$ such that for any partition $\mathcal{T}$ from this set and any tetrahedron $T \in \mathcal{T}$ we have

$$\operatorname{meas}_3 T \geqslant C(\operatorname{diam} T)^3, \tag{2.1}$$

where $\operatorname{diam} T$ is the diameter of T.

This condition guarantees that tetrahedra do not degenerate, i.e., the so-called minimum angle condition is fulfilled. The main idea of generating local nonobtuse tetrahedral partitions is exposed in the following theorem, whose proof is constructive. It is based on Coxeter's result that each path tetrahedron can be subdivided into three path tetrahedra (see [11]).

Theorem 2.4. *Let $ABCD$ be a path tetrahedron whose edges AB, BC, and CD are mutually perpendicular. Then there exists an infinite regular set of nonobtuse partitions of this tetrahedron into path tetrahedra that refine locally $ABCD$ in a neighborhood of the vertex A.*

Proof. Let P be the orthogonal projection of the point B onto the line AC. Obviously, P lies in the interior of the line segment AC, since ABC is a right triangle.

Further, let Q be the orthogonal projection of the point P onto the line AD. Since ACD is a right triangle, APD has an obtuse angle at P, and thus the point Q lies in the interior of the line segment AD.

We observe that the line segment BP is perpendicular to the face ACD. Therefore, BP is perpendicular to any line that is contained in the plane ACD. From this property we easily find that the original tetrahedron $ABCD$ can be decomposed into the following three path tetrahedra (see Fig. 3):

$$\begin{array}{lll} BPCD & \text{with} & BP \perp PC \perp CD \perp BP, \\ BPQD & \text{with} & BP \perp PQ \perp QD \perp BP, \\ AQPB & \text{with} & AQ \perp QP \perp PB \perp AQ. \end{array}$$

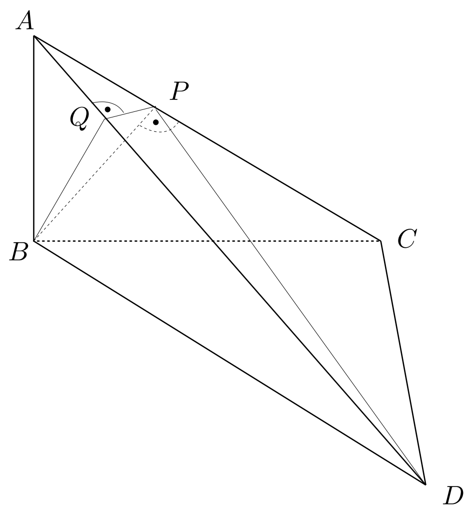

Figure 3. Partition of a path tetrahedron $ABCD$ into three path tetrahedra.

Now we decompose the last path subtetrahedron $AQPB$ again into three path subtetrahedra following the same rules as above. In this way we obtain a tetrahedron which is similar to the original tetrahedron $ABCD$, which will later help us to prove the regularity of the set of partitions.

So, let S be the orthogonal projection of the point Q onto the line AP, and let T be the orthogonal projection of the point S onto the line AB. Then the path tetrahedron $AQPB$ can be decomposed into the following three path subtetrahedra (see Fig. 4):

$$\begin{array}{lll} QSPB & \text{with} & QS \perp SP \perp PB \perp QS, \\ QSTB & \text{with} & QS \perp ST \perp TB \perp QS, \\ ATSQ & \text{with} & AT \perp TS \perp SQ \perp AT. \end{array}$$

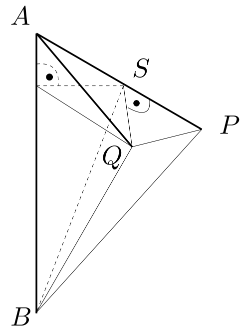

Figure 4. Partition of the path tetrahedron $ABQP$ into three path tetrahedra.

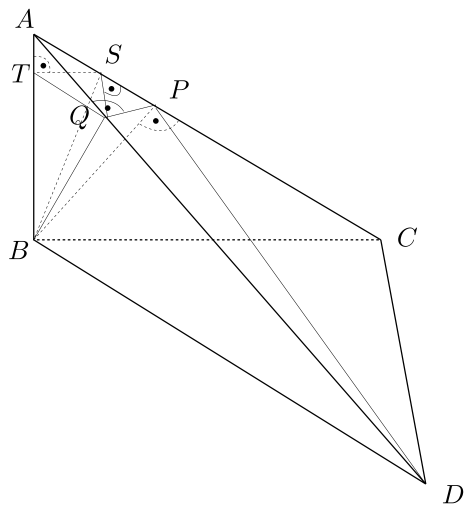

Figure 5. Partition of a path tetrahedron $ABCD$ into five path tetrahedra.

Consequently, the five path subtetrahedra $BPCD$, $BPQD$, $QSPB$, $QSTB$, and $ATSQ$ form a face-to-face partition of the original path tetrahedron $ABCD$ (see Fig. 5).

Since S is the orthogonal projection of Q onto the line AC, the line segments QS and DC are parallel. Similarly we find that TS and BC are parallel, since T is the orthogonal projection of S onto the line AB. From this we conclude that the face TSQ is parallel to BCD, and thus, the path subtetrahedron $ATSQ$ is similar to the original tetrahedron $ABCD$.

The subtetrahedron $ATSQ$ can be now decomposed into 5 subtetrahedra in a similar way (as $ABCD$), and thus we can get further refinement near the vertex A. By this recursive procedure, we obtain the required infinite set of face-to-face tetrahedral partitions and condition (2.1) will be satisfied, since any tetrahedron is similar to one of the five from Fig. 5. According to Proposition 2.2, each partition from this set is nonobtuse. □

3. Nonobtuse partitions locally refined near Fichera-like corners

In [19], we proposed an algorithm for the local nonobtuse tetrahedral partitioning of a cube in the neighborhood of one of its vertices. If several cubes meet at one point, then we can apply this algorithm to each one of them so that the whole partition remains face-to-face. For instance, in Fig. 6 we see local nonobtuse tetrahedral partitions of the polyhedral domain $\Omega = (-1,1)^3 \setminus [0,1)^3$, which represents a union of seven cubes. The concave (reentrant) corner of such a domain is called the *Fichera corner* or the *Fichera vertex* (see, e.g., [1], [2], [3], [14], [19]).

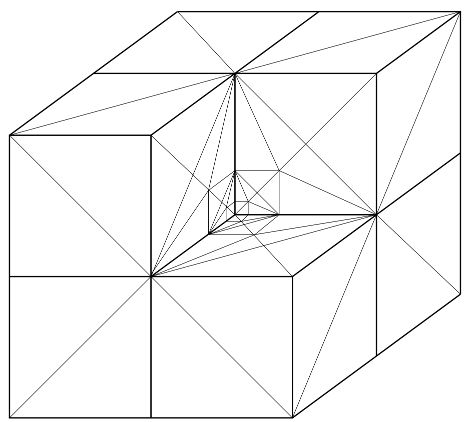

Figure 6. Locally refined nonobtuse partitions of the Fichera domain.

Actually, the algorithm from [19] can also be viewed as the following procedure: we first divide the cube into six path tetrahedra (cf. Fig. 7b), and further make a local nonobtuse tetrahedral partition of each of the path tetrahedra towards one of their two common vertices so that the overall partition of the whole cube always remains face-to-face.

If the algorithm from [19] is perceived as above, we immediately observe that the corresponding local partition of a single path tetrahedron coincides with the partition procedure presented in Section 2, if it is applied to a particular type of path tetrahedron—when its three mutually perpendicular edges are of the same length.

The comparison of the two above procedures immediately suggests the next generalization step, leading to a partitioning procedure for more general corners of polyhedral domains, which we will refer to as Fichera-like corners. In particular, we introduce sufficient conditions which make it possible to generate partitions that locally refine towards a given vertex A:

(i) Let $T_1, \ldots, T_k$ be tetrahedra from an initial partition that share a given vertex A belonging to the longest edge of each T_i, such that

(ii) T_1 is a path tetrahedron,

(iii) each T_i is a mirror image of any adjacent tetrahedron T_j with respect to their common triangular face $T_i \cap T_j$, $i, j \in \{1, \ldots, k\}$.

In Fig. 7, we observe three examples of clusters of path tetrahedra satisfying the above conditions (i)–(iii). Note that in Fig. 7a, the "lower" face is an equilateral triangle, in Fig. 7b, the cluster of tetrahedra form a cube, and in Fig. 7c, the "rectangular" face is a square.

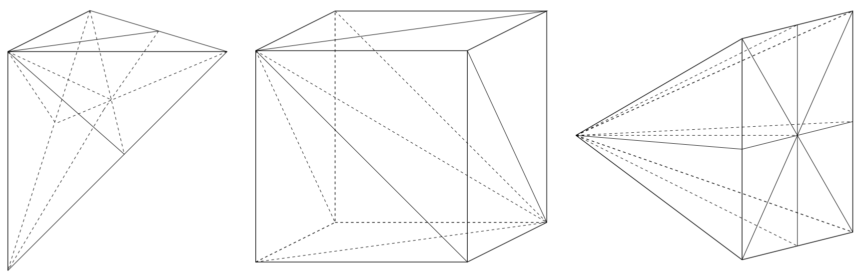

Figure 7. Clusters of path tetrahedra.

Now, let us consider a regular set of nonobtuse partitions of T_1. Its existence is guaranteed by Theorem 2.4. According to assumptions (i) and (iii), all tetrahedra adjacent to T_1 that share a face with T_1 (and hence also share the vertex A) are mirror images of T_1. Therefore, their partitions will be defined as mirror images of partitions of T_1. Similarly, we define partitions of all the other tetrahedra. Obviously, such a construction preserves the overall face-to-face property of the whole partition.

4. Numerical tests in domains with Fichera-like corners

In this section, we show the performance of the local mesh partitioning procedure applied to the solution of the Poisson equation with a nonhomogeneous Dirichlet boundary condition

$$\begin{aligned} -\Delta u &= f \quad \text{in } \Omega, \\ u &= \overline{u} \quad \text{on } \partial\Omega, \end{aligned}$$

where $\overline{u} \in H^{1/2}(\partial\Omega)$ is a given function and f will be defined below (see (4.2)).

The errors in Tabs. 1 and 3 are L^2-norms of the difference between the exact solution u and the computed finite element solution u_h over the domain Ω. The errors in Tabs. 2 and 4 are H^1-seminorms of the difference between the gradients of u and u_h

$$|u-u_h|_1 = \left(\int_\Omega |\nabla u - \nabla u_h|^2 \,\mathrm{d}x\right)^{1/2}.$$

In order to calculate the entries of the stiffness matrix and the load vector, we employ higher order numerical quadrature formulas on tetrahedra from [9], [10], [17], with 4, 11, and 24 integration points, which are exact for all polynomials of second, fourth, and sixth order, respectively. The integration points of these formulas are in the interior of each tetrahedron, which makes it possible to treat singularities at vertices of the solution itself (see, e.g., Example 4.2, where $u(0)=\infty$).

We shall consider solutions of the form

$$u(x) = \left(\sqrt{x_1^2+x_2^2+x_3^2}\right)^q, \tag{4.1}$$

where $x=(x_1,x_2,x_3)$ and q is a real number, in the unit sphere. Using the standard spherical coordinates (r,φ,θ) and the substitution theorem, we get for the H^1-norm of u and $q>-\frac{1}{2}$ that

$$\begin{aligned}\|u\|_1^2 &= \int_0^1\int_0^{2\pi}\int_0^{\pi}(r^{2q}+q^2r^{2q-2})r^2\sin\theta\,\mathrm{d}\theta\,\mathrm{d}\varphi\,\mathrm{d}r \\ &= 4\pi\int_0^1 (r^{2q+2}+q^2r^{2q})\,\mathrm{d}r = 4\pi\Big(\frac{1}{2q+3}+\frac{q^2}{2q+1}\Big)\in(0,\infty),\end{aligned}$$

and the triple integral is not finite whenever $q\leqslant -\frac{1}{2}$. The finiteness of $\|u\|_1$ remains valid if we replace the unit sphere by the union of several cubes which contain the origin $(0,0,0)$.

The right-hand side $f=-\Delta u$ corresponding to the solution (4.1) is

$$f(x) = -q(q+1)\frac{u(x)}{x_1^2+x_2^2+x_3^2}. \tag{4.2}$$

Example 4.1. Let $\Omega=((-1,1)^2\times(-1,0))\cup((0,1)^2\times[0,1))$, i.e., $\overline{\Omega}$ is the union of five unit cubes (see Fig. 8). We set $q=\frac{1}{2}$ and take $\overline{u}=u$ on $\partial\Omega$, where u is given by (4.1).

nodes	elements	4 pts	11 pts	24 pts
22	30	0.0533061	0.0577743	0.0579317
84	265	0.0153702	0.0162520	0.0162535
115	385	0.0153585	0.0162387	0.0162401
146	505	0.0153585	0.0162387	0.0162401

Table 1. L^2-norm of the error for Example 4.1.

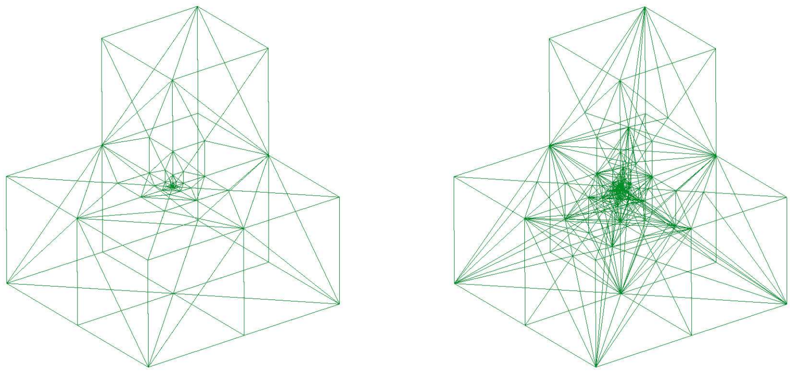

Figure 8. Local mesh partition of five cubes forming a Fichera-like corner after three refinement steps. The left figure only shows surface lines.

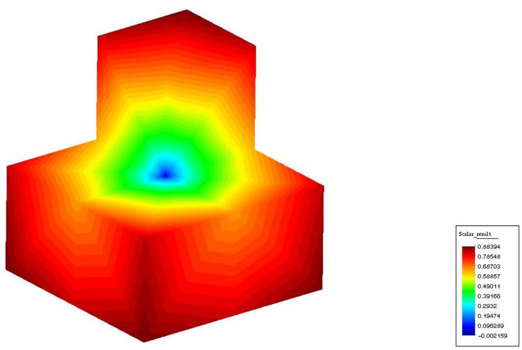

Figure 9. The solution of the Poisson equation for Example 4.1. A contour fill of u_h on a three times refined mesh is shown.

nodes	elements	4 pts	11 pts	24 pts
22	30	0.958325	1.028670	1.038700
84	265	0.590882	0.590969	0.590941
115	385	0.610457	0.610116	0.610112
146	505	0.713116	0.712898	0.712911

Table 2. H^1-seminorm of the error for Example 4.1.

Example 4.2. Let $\Omega = (-1,1)^3 \setminus [0,1)^3$, i.e., $\overline{\Omega}$ is the union of seven unit cubes (see Fig. 10) and the Fichera corner is in the origin (0,0,0). We set $q = -\frac{1}{4}$, and again take $\overline{u} = u$ on $\partial\Omega$. In this case, the solution itself has a singularity at the origin, see (4.1).

nodes	elements	4 pts	11 pts	24 pts
26	42	0.3705270	0.3708450	0.3697510
100	371	0.0196610	0.0210155	0.0209284
137	539	0.0115099	0.0141417	0.0141224
174	707	0.0107786	0.0135825	0.0135698

Table 3. L^2-norm of the error for Example 4.2.

nodes	elements	4 pts	11 pts	24 pts
26	42	1.97317	2.37207	2.54099
100	371	1.43409	1.45116	1.44991
137	539	2.79540	2.80079	2.80042
174	707	6.35086	6.35945	6.35787

Table 4. H^1-seminorm of the error for Example 4.2.

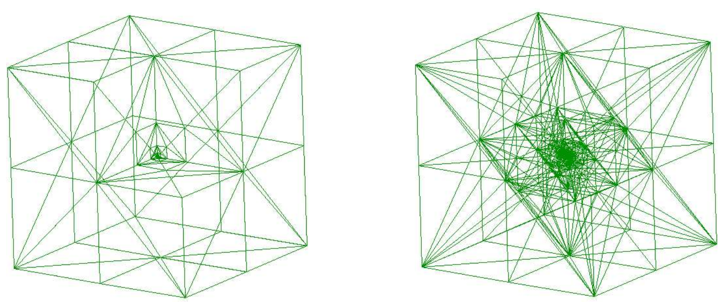

Figure 10. Local mesh partition of seven cubes forming a Fichera-like corner after three refinement steps. The left figure only shows the surface lines.

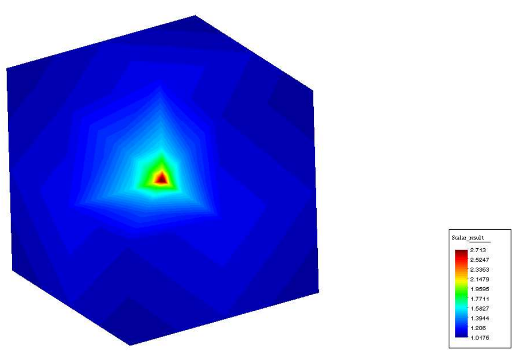

Figure 11. The solution of the Poisson equation for Example 4.2. A contour fill of u_h on a three times refined mesh is shown.

From Tables 1–4 we observe that numerical integration formulae with 11 and 24 nodes yield almost the same results which only slightly differ from those obtained by the four node formula. We also see that a proper numerical treatment of the essential singularity from Example 4.2 is very difficult to perform.

Acknowledgement. We would like to express our sincere gratitude to Thomas Apel and Jan Brandts for their valuable comments on this paper.

References

[1] *T. Apel*: Anisotropic Finite Elements: Local Estimates and Applications. Advances in Numer. Math. B. G. Teubner, Leipzig, 1999.

[2] *T. Apel, F. Milde*: Comparison of several mesh refinement strategies near edges. Commun. Numer. Methods Eng. *12* (1996), 373–381.

[3] *T. Apel, S. Nicaise*: The finite element method with anisotropic mesh grading for elliptic problems in domains with corners and edges. Math. Methods Appl. Sci. *21* (1998), 519–549.

[4] *O. Axelsson, V. A. Barker*: Finite Element Solution of Boundary Value Problems. Theory and Computation. Academic Press, Orlando, 1984.

[5] *M. Bern, P. Chew, D. Eppstein, and J. Ruppert*: Dihedral bounds for mesh generation in high dimensions. Proc. of the 6th Annual ACM-SIAM Symposium on Discrete Algorithms (San Francisco, CA, 1995). SIAM, Philadelphia, 1995, pp. 189–196.

[6] *F. Bornemann, B. Erdmann, and R. Kornhuber*: Adaptive multilevel methods in three space dimensions. Int. J. Numer. Methods Eng. *36* (1993), 3187–3203.

[7] *E. Bänsch*: Local mesh refinement in 2 and 3 dimensions. IMPACT Comput. Sci. Eng. *3* (1991), 181–191.

[8] *L. Collatz*: Numerische Behandlung von Differentialgleichungen. Springer-Verlag, Berlin-Göttingen-Heidelberg, 1951.

[9] *R. Cools*: Monomial cubature rules since "Stroud": A compilation. II. J. Comput. Appl. Math. *112* (1999), 21–27.

[10] *R. Cools, P. Rabinowitz*: Monomial cubature rules since "Stroud": A compilation. J. Comput. Appl. Math. *48* (1993), 309–326.

[11] *H. S. M. Coxeter*: Trisecting an orthoscheme. Comput. Math. Appl. *17* (1989), 59–71.

[12] *M. Dauge*: Elliptic Boundary Value Problems on Corner Domains. Lect. Notes Math., Vol. 1341. Springer-Verlag, Berlin, 1988.

[13] *M. Feistauer, J. Felcman, M. Rokyta, and Z. Vlášek*: Finite-element solution of flow problems with trailing conditions. J. Comput. Appl. Math. *44* (1992), 131–165.

[14] *G. Fichera*: Numerical and Quantitative Analysis. Surveys and Reference Works in Mathematics, Vol. 3. Pitman (Advanced Publishing Program), London-San Francisco-Melbourne, 1978.

[15] *H. Fujii*: Some remarks on finite element analysis of time-dependent field problems. Theory Pract. Finite Elem. Struct. Analysis. Univ. Tokyo Press, Tokyo, 1973, pp. 91–106.

[16] *B. Q. Guo*: The *h-p* version of the finite element method for solving boundary value problems in polyhedral domains. Boundary Value Problems and Integral Equations in Nonsmooth Domains (Luminy, 1993). Lect. Notes Pure Appl. Math., Vol. 167 (M. Costabel, M. Dauge, and C. Nicaise, eds.). Marcel Dekker, New York, 1995, pp. 101–120.

[17] *P. Keast*: Moderate-degree tetrahedral quadrature formulas. Comput. Methods Appl. Mech. Eng. *55* (1986), 339–348.

[18] *S. Korotov, M. Křížek*: Acute type refinements of tetrahedral partitions of polyhedral domains. SIAM J. Numer. Anal. *39* (2001), 724–733.
[19] *S. Korotov, M. Křížek*: Local nonobtuse tetrahedral refinements of a cube. Appl. Math. Lett. *16* (2003), 1101–1104.
[20] *I. Kossaczký*: A recursive approach to local mesh refinement in two and three dimensions. J. Comput. Appl. Math. *55* (1994), 275–288.
[21] *M. Křížek, L. Liu*: On the maximum and comparison principles for a steady-state nonlinear heat conduction problem. Z. Angew. Math. Mech. *83* (2003), 559–563.
[22] *M. Křížek, Qun Lin*: On diagonal dominance of stiffness matrices in 3D. East-West J. Numer. Math. *3* (1995), 59–69.
[23] *M. Křížek, T. Strouboulis*: How to generate local refinements of unstructured tetrahedral meshes satisfying a regularity ball condition. Numer. Methods Partial Differ. Equations *13* (1997), 201–214.
[24] *J. M. Maubach*: Local bisection refinement for n-simplicial grids generated by reflection. SIAM J. Sci. Comput. *16* (1995), 210–227.
[25] *M. Picasso*: Numerical study of the effectivity index for an anisotropic error indicator based on Zienkiewicz-Zhu error estimator. Commun. Numer. Methods Eng. *19* (2003), 13–23.
[26] *M. Picasso*: An anisotropic error indicator based on Zienkiewicz-Zhu error estimator: Application to elliptic and parabolic problems. SIAM J. Sci. Comput. *24* (2003), 1328–1355.
[27] *A. Plaza, G. F. Carey*: Local refinement of simplicial grids based on the skeleton. Appl. Numer. Math. *32* (2000), 195–218.
[28] *H. Schmitz, K. Volk, and W. Wendland*: Three-dimensional singularities of elastic fields near vertices. Numer. Methods Partial Differ. Equations *9* (1993), 323–337.
[29] *R. S. Varga*: Matrix iterative analysis. Prentice-Hall, New Jersey, 1962.

Authors' addresses: *L. Beilina*, Department of Mathematics, University of Basel, Rheinsprung 21, CH-4051 Basel, Switzerland, e-mail: `beilina@math.unibas.ch`; *S. Korotov*, Helsinki University of Technology, Institute of Mathematics, P.O. Box 1100, FI-02015 Espoo, Finland, e-mail: `sergey.korotov@hut.fi`; *Michal Křížek*, Mathematical Institute of the Academy of Sciences of the Czech Republic, Žitná 25, CZ–115 67 Praha 1, Czech Republic, e-mail: `krizek@math.cas.cz`.